Received: November 1, 2016 | Accepted: November 22, 2016 | Web Released: November 30, 2016 CL-160994

Editor's Choice

Open-circuit Voltage Loss in $CH_3NH_3SnI_3$ Perovskite Solar Cells


H. Ohkita

Hyung Do Kim,[1] Yoshihiro Miyamoto,[2] Hirofumi Kubota,[2] Toshihiko Yamanari,[2] and Hideo Ohkita*[1]
[1]*Department of Polymer Chemistry, Graduate School of Engineering, Kyoto University, Katsura, Nishikyo, Kyoto 615-8510*
[2]*Chemical Materials Evaluation and Research Base (CEREBA), Tsukuba, Ibaraki 305-8565*

(E-mail: ohkita@photo.polym.kyoto-u.ac.jp)

Organic–inorganic perovskite solar cells based on tin halides exhibit a small open-circuit voltage (V_{OC}) because of a large photon energy loss from band-gap energy, as large as 0.8–1.0 eV. In this study, we discussed the origin of the V_{OC} loss in $CH_3NH_3SnI_3$-based devices by measuring the temperature dependence of V_{OC}. As a result, we found that the large loss in V_{OC} is mainly due to the surface recombination at the interface rather than the bulk recombination in the perovskites.

Keywords: Perovskite solar cell | Tin halide | Surface recombination

Organic–inorganic perovskite solar cells based on lead halides ($CH_3NH_3PbI_{3-x}Cl_x$) have attracted much attention of many researchers owing to their superior optical and electronic properties, such as high absorption coefficient and charge carrier mobility, small exciton binding energy, and long diffusion length of charge carriers.[1–3] Moreover, they have shown a steep increase in the power conversion efficiency (PCE) from 3.8% in 2009[4] to more than 22% in 2016[5,6] and hence are recently considered as a promising next-generation photovoltaic device. However, the use of toxic material (Pb) still remains a major obstacle for the commercialization of these devices. Thus, it is highly desirable for environmental friendly devices to replace lead(II) with other nontoxic metal elements, such as germanium(II), tin(II), and bismuth(III).[7–12]

Very recently, several groups have successfully fabricated organic–inorganic perovskites solar cells based on tin halides ($CH_3NH_3SnI_3$), which yields the best PCE in the range of 5–6%.[8,11,12] However, the device performance of tin-based perovskite solar cells still lags far behind that of lead-based counterparts. In particular, the open-circuit voltage (V_{OC}) is typically much smaller than the band-gap energy (E_g). In other words, the photon energy loss (E_{loss}) from E_g is as large as 0.8–1.0 eV, which is larger by 0.3–0.5 eV than that for lead-based devices.[13–15] Hence, it is highly required to study the origin of the V_{OC} loss for further improvements in the device performance of tin-based perovskite solar cells.

Herein, we have fabricated the $CH_3NH_3SnI_3$-based solar cells with a layer structure as shown in Figure 1a, and studied the origin of the photon energy loss $E_{loss} = E_g - qV_{OC}$ (q is the elementary charge) by measuring the temperature dependence of V_{OC}. As a result, we found that the dominant recombination mechanism in these devices is the surface recombination at the interface rather than the bulk recombination of the perovskite layer, eventually resulting in a large loss in V_{OC}.

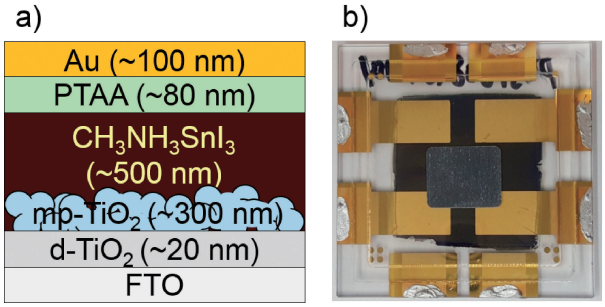

Figure 1. a) Schematic illustration of the device structure of tin-based perovskite solar cells with a layer structure of FTO/dense TiO_2 (d-TiO_2)/mesoporous TiO_2 (mp-TiO_2):$CH_3NH_3SnI_3$/poly(triarylamine) (PTAA)/Au and b) a photographic top view of an encapsulated solar cell. The gray square sheet at the center is a water getter.

Organic–inorganic perovskite solar cells based on tin halides ($CH_3NH_3SnI_3$) were fabricated as follows. A 20-nm-thick layer of dense TiO_2 (d-TiO_2) was coated onto an F-doped SnO_2 (FTO; Asahi Glass) substrate by plasma-enhanced atomic layer deposition (a source material was titanium(IV) isopropoxide (TTIP)). Mesoporous TiO_2 (mp-TiO_2) films were deposited onto the d-TiO_2/FTO substrate by spin-coating a TiO_2 paste (Nikki Syokubai Kasei, PST-18NR) diluted by ethanol (1:3 by weight). The samples were calcined at 500 °C for 1 h. The samples were transferred to a nitrogen-filled glove box. Methylammonium iodide (CH_3NH_3I), SnI_2, and SnF_2 were dissolved in dimethyl sulfoxide (DMSO) at a molar ratio of 1:1:0.2. The concentration of $CH_3NH_3SnI_3$ was 39.9 wt %. The mixed solution was then coated onto the mp-TiO_2/d-TiO_2/FTO substrate by spin-coating at 3000 rpm for 60 s. During the spin-coating procedure, toluene was dropped onto the substrate, and dried on a hot plate at 65 °C for 1 h. A poly(triarylamine) (PTAA)/toluene (15 mg/1 mL) solution with added 7.5 µL Li-bis(trifluoromethanesulfonyl)imide (Li-TFSI)/acetonitrile (170 mg/1 mL) and 7.5 µL *tert*-butylpyridine (*t*-BP) (1 mL *t*-BP/1 mL acetonitrile) was spin-coated on the $CH_3NH_3SnI_3$/mp-TiO_2/d-TiO_2/FTO substrate at 3000 rpm for 60 s and dried on a hot plate at 65 °C for 5 min. A gold electrode was deposited by vacuum evaporation. The active area of the cell was 0.49 cm^2. Figure 1a shows the thickness of each layer in the device fabricated. The device was encapsulated by a glass cap using a UV cure resin and a water getter was inserted into the space between the substrate and the glass cap, as shown in Figure 1b.

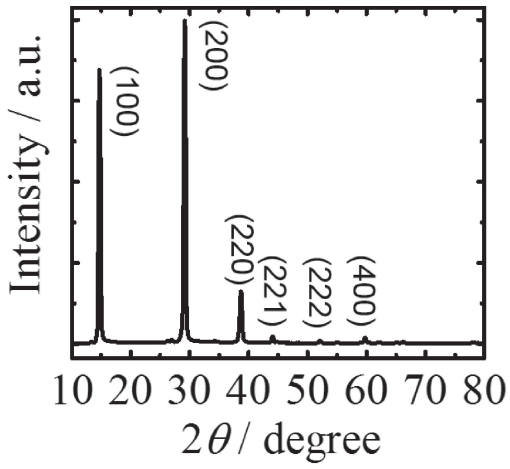

Figure 2. X-ray diffraction (XRD) pattern for $CH_3NH_3SnI_3$ perovskites fabricated from DMSO.

Current density and voltage (J–V) characteristics were measured with a direct-current (DC) voltage and current source/monitor (Keithley, 2611B) in the dark and under the illumination with AM1.5G simulated solar light with 100 mW cm^{-2}. The light intensity was corrected with a calibrated silicon photodiode reference cell (Bunkoh-Keiki, BS-520). Temperature dependence of the J–V characteristics was measured with a DC voltage and current source/monitor (Advantest, R6243) in a vacuum prober system (ALS Technology, VPS3-50) under the illumination from a 100 W Xe lamp (Asahi Spectra, LAX-C100) equipped with a uniform illumination lens unit (Asahi Spectra, RLQL80-0.5). The temperature was controlled by the cryocooler (Twinbird Corp., SC-UF01) and monitored by the temperature controller (Panasonic, KT2). The external quantum efficiency (EQE) spectra were measured with a spectral response measurement system (Bunko-Keiki Co., ECT-250D). The power of the incident monochromatic light was kept under 0.05 mW cm^{-2}, which was measured by a calibrated silicon reference cell. All encapsulated devices were measured with a metal mask to give an active area of 0.09 cm^2.

Figure 2 shows the X-ray diffraction (XRD) pattern for $CH_3NH_3SnI_3$ perovskites fabricated from DMSO. As shown in the figure, sharp diffraction peaks were observed at 14.7, 29.2, 38.7, 44.1, 52.1, and 59.8°, which are ascribed to the (100), (200), (220), (221), (222), and (400) planes, respectively. These peaks indicate the pseudocubic phase of $CH_3NH_3SnI_3$ perovskites, which is in good agreement with the previous literatures.[8,11,12,16,17]

Figure 3a shows the J–V characteristics of $CH_3NH_3SnI_3$ perovskite solar cells, which were measured from −0.50 to 0.70 V (forward scan) and from 0.70 to −0.50 V (reverse scan) with a delay time of 1 s under 100 mW cm^{-2} AM 1.5G solar illumination condition. Note that the histograms of device parameters are summarized in Figure S1 (see Supporting Information (SI)). As summarized in Table 1, the short-circuit current density (J_{SC}) was as large as 26 mA cm^{-2}, which is slightly larger than that (ca. 24 mA cm^{-2}) of lead-based counterparts.[5,15] This is because $CH_3NH_3SnI_3$ perovskites can absorb many more photons in the near-infrared region up to 1000 nm. Such a high J_{SC} obtained from the J–V curve is in good

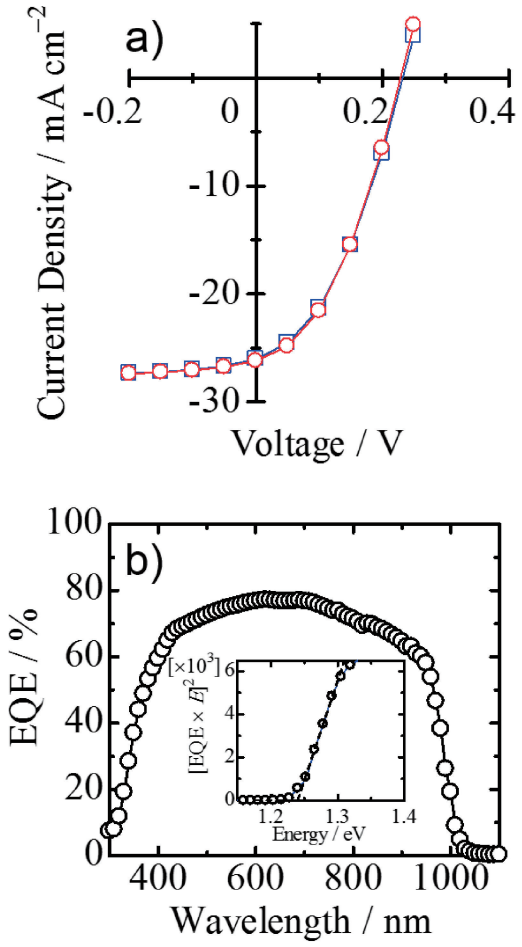

Figure 3. a) J–V characteristics of $CH_3NH_3SnI_3$ perovskite solar cells: forward scan (blue open squares) and reverse scan (red open circles). b) EQE spectra of $CH_3NH_3SnI_3$ perovskite solar cells. The inset shows $[E \times \mathrm{EQE}]^2$ plotted against the photon energy E of this device.

Table 1. Photovoltaic parameters of $CH_3NH_3SnI_3$ perovskite solar cell employed in this study

	J_{SC}/mA cm^{-2}	V_{OC}/V	FF	PCE/%
Forward	26.0	0.232	0.386	2.33
Reverse	26.2	0.229	0.387	2.32

agreement with that calculated from the EQE and solar spectra, as shown in Figure 3b. On the other hand, V_{OC} was as small as 0.23 V and a fill factor (FF) was as small as 0.39, both of which are significantly smaller than those of lead-based counterparts.[5,15] Note that no J–V hysteresis was observed for all the devices studied. These findings clearly indicate that the small V_{OC} and FF are the major loss in $CH_3NH_3SnI_3$ perovskite solar cells.

To estimate the voltage loss, we evaluated the E_g of the $CH_3NH_3SnI_3$ perovskite from the EQE spectra.[13,18] From the x-axis intercept of $[E \times \mathrm{EQE}]^2$ plotted against the photon energy E, as shown in the inset of Figure 3b, E_g was estimated to be 1.23 eV, which is in good agreement with previous reports.[8,12]

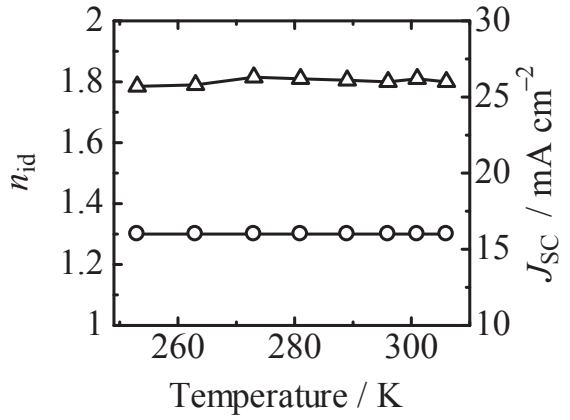

Figure 4. Temperature dependence of n_{id} (open circles) and J_{SC} (open triangles).

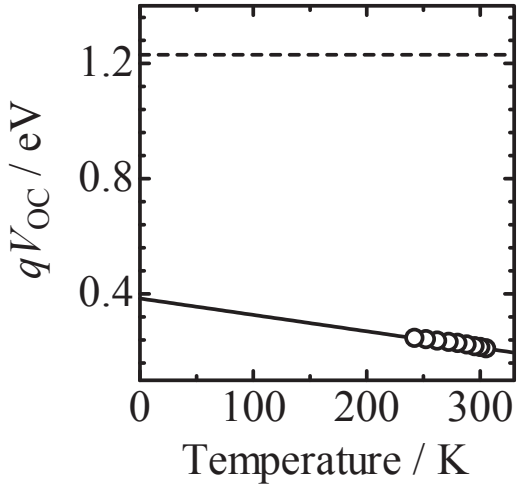

Figure 5. Temperature dependence of qV_{OC} for $CH_3NH_3SnI_3$ perovskite solar cells. The solid line is a linear fit to experimental data with eq 3. The broken line represents a band-gap energy (E_g).

Consequently, the photon energy loss E_{loss} is estimated to be as large as 1.0 eV. This is larger by 0.5 eV than that reported for $CH_3NH_3PbI_3$ perovskite solar cells.[13–15] Therefore, there should be an additional recombination loss channel in $CH_3NH_3SnI_3$ perovskite solar cells.

We next measured the temperature dependence of *J–V* characteristics to discuss the origin of voltage loss in tin-based devices. On the basis of the equivalent circuit model under typical condition, V_{OC} is given by

$$V_{OC} = \frac{n_{id}k_BT}{q}\ln\left(\frac{J_{SC}}{J_0}\right) \quad (1)$$

where n_{id} is the ideality factor, k_B is the Boltzmann constant, T is the temperature, and J_0 is the saturation current density at reverse bias. As reported previously,[19] J_0 can be given by the Arrhenius equation

$$J_0 = J_{00}\exp\left(-\frac{E_a}{n_{id}k_BT}\right) \quad (2)$$

where J_{00} is the pre-exponential factor and E_a is the activation energy of the diode. From these equations, eq 3 is obtained.

$$qV_{OC} = E_a - n_{id}k_BT\ln\left(\frac{J_{00}}{J_{SC}}\right) \quad (3)$$

Here, n_{id} was estimated from a slope in V_{OC} plotted against the logarithm of J_{SC} on the basis of eq 1.[19] As shown in Figure 4, the n_{id} and J_{SC} values were ca. 1.3 and ca. 26 mA cm^{-2}, respectively, both of which were independent of temperature over the temperature range measured. Consequently, E_a can be evaluated to be 0.39 eV from a linear extrapolation at 0 K, as shown in Figure 5. On the other hand, as shown in Figure 5, the temperature dependent energy loss $E_a - qV_{OC}$ was as small as 0.16 eV even at room temperature.

Finally, we discuss the origin of voltage loss in tin-based devices on the basis of the results obtained. As reported previously, the activation energy of the diode E_a is nearly equal to E_g for bulk recombination in the absorber layer such as direct recombination and Shockley–Read–Hall (SRH) recombination.[20–25] However, this is not the case for our $CH_3NH_3SnI_3$ solar cells, because E_a is much smaller than E_g. Rather, the smaller E_a is attributed to the surface recombination at the buffer/absorber interface.[22,24–26] In such case, E_a is nearly equal to the barrier height Φ_b at the interface, which is typically smaller than E_g ($\Phi_b < E_g$). In addition, the temperature-dependent voltage loss (0.16 eV) that we observed cannot be explained in terms of the bulk recombination such as direct and trap-assisted SRH recombination. If the bulk recombination were dominant, the temperature-dependent voltage loss would be larger than 0.3 eV at least because of the thermodynamically inevitable loss in V_{OC} due to an intense absorption coefficient (10^4–10^5 cm^{-1}).[15,17,27–30] Furthermore, an additional voltage loss would be involved because of the nonradiative recombination, which is typically in the range of 0.2–0.3 eV as reported previously.[15,29–31] In addition, the ideality factor n_{id} as small as ca. 1.3 also suggests that dominant recombination is surface recombination rather than trap-assisted recombination in our $CH_3NH_3SnI_3$ solar cells.[23,32] We therefore conclude that the primary voltage loss mechanism in $CH_3NH_3SnI_3$ perovskite solar cells is the surface recombination at the interface rather than bulk recombination in the perovskite absorber layer. This is the origin for the large photon energy loss ($E_{loss} = 1.0$ eV). This finding suggests that $CH_3NH_3SnI_3$ perovskite devices are controlled by surface recombination at the interface rather than the bulk recombination of perovskite layer, which is the primary cause of the large loss in V_{OC}.

In summary, we studied the origin of voltage loss in tin-based perovskite solar cells with a layer structure of FTO/d-TiO_2/mp-TiO_2:$CH_3NH_3SnI_3$/PTAA/Au. The device exhibited a significantly small V_{OC} of 0.23 V, which is far below the optical band gap $E_g = 1.23$ eV obtained from the EQE spectra. Thus, the photon energy loss is evaluated to be as large as $E_{loss} = 1.0$ eV, which is almost two times larger than that reported for $CH_3NH_3PbI_3$ perovskite solar cells. In order to discuss the dominant recombination mechanism in the cell, we measured the temperature dependence of V_{OC}. From a linear extrapolation at 0 K, the activation energy of the diode E_a was evaluated to be 0.39 eV, which is significantly smaller than $E_g = 1.23$ eV. In addition, the temperature-dependent energy loss $E_a - qV_{OC}$ was

as small as 0.16 eV even at room temperature. From a slope in V_{OC} plotted against the logarithm of J_{SC}, n_{id} for $CH_3NH_3SnI_3$ perovskite solar cells was also evaluated to be ca. 1.3, which is closer to unity than 2. We therefore conclude that such a large energy loss is primarily ascribed to the surface recombination at the interface rather than the bulk recombination in the perovskite layer. In other words, the surface recombination at the interface should be suppressed for further improvements of tin-based perovskite solar cells.

This study is based on the results obtained from a project commissioned by the New Energy and Industrial Technology Development Organization (NEDO).

Supporting Information is available on http://dx.doi.org/10.1246/cl.160994.

References

1 S. D. Stranks, G. E. Eperon, G. Grancini, C. Menelaou, M. J. P. Alcocer, T. Leijtens, L. M. Herz, A. Petrozza, H. J. Snaith, *Science* **2013**, *342*, 341.
2 C. Wehrenfennig, G. E. Eperon, M. B. Johnston, H. J. Snaith, L. M. Herz, *Adv. Mater.* **2014**, *26*, 1584.
3 M. Saba, M. Cadelano, D. Marongiu, F. Chen, V. Sarritzu, N. Sestu, C. Figus, M. Aresti, R. Piras, A. G. Lehmann, C. Cannas, A. Musinu, F. Quochi, A. Mura, G. Bongiovanni, *Nat. Commun.* **2014**, *5*, 5049.
4 A. Kojima, K. Teshima, Y. Shirai, T. Miyasaka, *J. Am. Chem. Soc.* **2009**, *131*, 6050.
5 T. Miyasaka, *Chem. Lett.* **2015**, *44*, 720.
6 N. G. Park, M. Grätzel, T. Miyasaka, K. Zhu, K. Emery, *Nat. Energy* **2016**, *1*, 16152.
7 T. Krishnamoorthy, H. Ding, C. Yan, W. L. Leong, T. Baikie, Z. Zhang, M. Sherburne, S. Li, M. Asta, N. Mathews, S. G. Mhaisalkar, *J. Mater. Chem. A* **2015**, *3*, 23829.
8 N. K. Noel, S. D. Stranks, A. Abate, C. Wehrenfennig, S. Guarnera, A.-A. Haghighirad, A. Sadhanala, G. E. Eperon, S. K. Pathak, M. B. Johnston, A. Petrozza, L. M. Herz, H. J. Snaith, *Energy Environ. Sci.* **2014**, *7*, 3061.
9 Y. Ogomi, A. Morita, S. Tsukamoto, T. Saitho, N. Fujikawa, Q. Shen, T. Toyoda, K. Yoshino, S. S. Pandey, T. Ma, S. Hayase, *J. Phys. Chem. Lett.* **2014**, *5*, 1004.
10 B.-W. Park, B. Philippe, X. Zhang, H. Rensmo, G. Boschloo, E. M. J. Johansson, *Adv. Mater.* **2015**, *27*, 6806.
11 W. Liao, D. Zhao, Y. Yu, C. R. Grice, C. Wang, A. J. Cimaroli, P. Schulz, W. Meng, K. Zhu, R.-G. Xiong, Y. Yan, *Adv. Mater.* **2016**, *28*, 9333.
12 T. Yokoyama, D. H. Cao, C. C. Stoumpos, T.-B. Song, Y. Sato, S. Aramaki, M. G. Kanatzidis, *J. Phys. Chem. Lett.* **2016**, *7*, 776.
13 W. L. Leong, Z.-E. Ooi, D. Sabba, C. Yi, S. M. Zakeeruddin, M. Grätzel, J. M. Gordon, E. A. Katz, N. Mathews, *Adv. Mater.* **2016**, *28*, 2439.
14 C. Huang, C. Liu, Y. Di, W. Li, F. Liu, L. Jiang, J. Li, X. Hao, H. Huang, *ACS Appl. Mater. Interfaces* **2016**, *8*, 8520.
15 H. D. Kim, H. Ohkita, H. Benten, S. Ito, *Adv. Mater.* **2016**, *28*, 917.
16 H. Hoshi, N. Shigeeda, T. Dai, *Mater. Lett.* **2016**, *183*, 391.
17 Y. Yu, D. Zhao, C. R. Grice, W. Meng, C. Wang, W. Liao, A. J. Cimaroli, H. Zhang, K. Zhu, Y. Yan, *RSC Adv.* **2016**, *6*, 90248.
18 T. K. Todorov, O. Gunawan, T. Gokmen, D. B. Mitzi, *Prog. Photovoltaics Res. Appl.* **2013**, *21*, 82.
19 S. M. Sze, *Physics of Semiconductor Devices*, 2nd ed., Wiley, New York, **1981**.
20 K. Vandewal, K. Tvingstedt, A. Gadisa, O. Inganäs, J. V. Manca, *Phys. Rev. B* **2010**, *81*, 125204.
21 D. Bozyigit, W. M. M. Lin, N. Yazdani, O. Yarema, V. Wood, *Nat. Commun.* **2015**, *6*, 6180.
22 V. Nadenau, U. Rau, A. Jasenek, H. W. Schock, *J. Appl. Phys.* **2000**, *87*, 584.
23 S. Wheeler, F. Deledalle, N. Tokmoldin, T. Kirchartz, J. Nelson, J. R. Durrant, *Phys. Rev. Appl.* **2015**, *4*, 024020.
24 U. Rau, H. W. Schock, *Appl. Phys. A: Mater. Sci. Process.* **1999**, *69*, 131.
25 M. Turcu, O. Pakma, U. Rau, *Appl. Phys. Lett.* **2002**, *80*, 2598.
26 X. Zheng, B. Chen, M. Yang, C. Wu, B. Orler, R. B. Moore, K. Zhu, S. Priya, *ACS Energy Lett.* **2016**, *1*, 424.
27 W. Shockley, H. J. Queisser, *J. Appl. Phys.* **1961**, *32*, 510.
28 M. Gruber, J. Wagner, K. Klein, U. Hörmann, A. Opitz, M. Stutzmann, W. Brütting, *Adv. Energy Mater.* **2012**, *2*, 1100.
29 D. Bi, W. Tress, M. I. Dar, P. Gao, J. Luo, C. Renevier, K. Schenk, A. Abate, F. Giordano, J.-P. C. Baena, J.-D. Decoppet, S. M. Zakeeruddin, M. K. Nazeeruddin, M. Grätzel, A. Hagfeldt, *Sci. Adv.* **2016**, *2*, e1501170.
30 W. Tress, N. Marinova, O. Inganäs, M. K. Nazeeruddin, S. M. Zakeeruddin, M. Grätzel, *Adv. Energy Mater.* **2015**, *5*, 1400812.
31 G.-J. A. H. Wetzelaer, M. Scheepers, A. M. Sempere, C. Momblona, J. Ávila, H. J. Bolink, *Adv. Mater.* **2015**, *27*, 1837.
32 C. Sah, R. N. Noyce, W. Shockley, *Proc. IRE* **1957**, *45*, 1228.